Original article

Nuclear Medicine Communications

Obtaining quantitative global tumoral state indicators based on whole-body PET/CT scans: a breast cancer case study

Frederic Sampedro[a], Anna Domenech[c] and Sergio Escalera[b,d]

Objectives **In this work we address the need for the computation of quantitative global tumoral state indicators from oncological whole-body PET/computed tomography scans. The combination of such indicators with other oncological information such as tumor markers or biopsy results would prove useful in oncological decision-making scenarios.**

Materials and methods **From an ordering of 100 breast cancer patients on the basis of oncological state through visual analysis by a consensus of nuclear medicine specialists, a set of numerical indicators computed from image analysis of the PET/computed tomography scan is presented, which attempts to summarize a patient's oncological state in a quantitative manner taking into consideration the total tumor volume, aggressiveness, and spread.**

Results **Results obtained by comparative analysis of the proposed indicators with respect to the experts' evaluation show up to 87% Pearson's correlation coefficient when providing expert-guided PET metabolic tumor volume segmentation and 64% correlation when using completely automatic image analysis techniques.**

Conclusion **Global quantitative tumor information obtained by whole-body PET/CT image analysis can prove useful in clinical nuclear medicine settings and oncological decision-making scenarios. The completely automatic computation of such indicators would improve its impact as time efficiency and specialist independence would be achieved.** ***Nucl Med Commun*** **35:362–371 © 2014 Wolters Kluwer Health | Lippincott Williams & Wilkins.**

Nuclear Medicine Communications 2014, **35**:362–371

Keywords: image analysis, oncology, PET, quantification

[a]Faculty of Medicine, [b]Computer Vision Center, Autonomous University of Barcelona, [c]Nuclear Medicine Department, Hospital de Sant Pau and [d]Faculty of Mathematics, University of Barcelona, Barcelona, Spain

Correspondence to Frederic Sampedro, MSc, Faculty of Medicine, Autonomous University of Barcelona, Barcelona 08193, Spain
Tel: +34 699 805 231; fax: +34 934 037 151;
e-mail: fredsampedro@gmail.com

Received 21 October 2013 **Revised** 20 November 2013
Accepted 25 November 2013

Introduction and related work

^{18}F-fluorodeoxyglucose (^{18}F-FDG) PET/computed tomography (PET/CT) has become a standard imaging method for the staging, restaging, and monitoring of treatment response in a variety of tumors. By injecting the ^{18}F-FDG radiopharmaceutical into the patient, a metabolic image of the whole body, measured in standard uptake value (SUV) units, is acquired. This metabolic image is obtained in combination with a coregistered CT scan that provides higher anatomical resolution (in Hounsfield units, HU).

Whole-body (WB) PET/CT scans are a valuable tool for cancer detection and can be used to evaluate the spread of cancer throughout the patient's body [1,2]. The current analysis of WB PET/CT scans is mainly visual; nuclear medicine physicians build a descriptive report about their findings regarding the possible location of cancer and its metastases.

Local quantitative tumor lesion information, such as its mean and maximum uptake value (SUV_{mean}, SUV_{max}) and diameter, is usually included in the report. Global quantitative information, such as the whole-body metabolic tumor volume (WBMTV) and total lesion glycolysis (TLG), is usually not included in the report, although they have been proven to be clinically relevant as independent prognostic markers [3–7]. This may be partly because the measurement of these parameters, which currently requires an expert-guided manual or semiautomatic tumor segmentation from the PET scan, is highly time consuming and therefore not practical in a clinical setting. It may also be because the usefulness of this time-inefficient measurement has not been fully determined [7].

In this work we address the computation of global quantitative indicators from WB PET/CT scans that reflect the patient's oncological state. This type of indicator is referred to as PET Global Oncological State Indicator (PGOSI) hereon. Here, we consider that the oncological state of a patient is deduced in a qualitative manner from the expert-based visual analysis of WB PET images and is related to the quantity of tumor present in the body as well as its aggressiveness and spread. Clinical nuclear medicine experts agree on the need for such a quantitative indicator that, when combined with complementary oncological indicators such as tumor markers

0143-3636 © 2014 Wolters Kluwer Health | Lippincott Williams & Wilkins DOI: 10.1097/MNM.0000000000000067

or biopsy results, would prove a valuable tool for oncological decision making [1,2]. WBMTV and TLG can be considered examples of PGOSI. Some conceptual limitations of these indicators as well as new indicator proposals that try to overcome them are presented in the subsequent sections.

In this scenario, defining a gold standard for assessing the performance of any proposed PGOSI is a complex task. It could be argued that an appropriate choice would be to compare the PGOSI results with other oncological clinical variables such as biopsy results, TNM staging [8], tumor markers, or *N*-year survival rates. However, we consider that none of these variables appropriately model what our PGOSI proposal is intended for: biopsy results are only conclusive about a single anatomical location and do not relate directly to the total tumor quantity and spread within the patient's whole body; TNM staging does give an insight into the tumor quantity and spread but in a categorical manner, and hence it could be argued that two patients may possess slightly different oncological states albeit belonging to the same TNM category; tumor marker results may be independent of PET/CT observations depending on the type of tumor and its stage, and *N*-year survival rates may not be appropriate for comparison with PGOSI results as patients may undergo different treatments and suffer from other nononcological pathologies.

Note that in the related scenario of PET follow-up evaluation, in which two time consecutive PET/CT scans are compared to address therapy response, treatment outcome parameters can be successfully used as the gold standard to address the performance of the proposed quantitative indicators obtained by the pair of PET/CT scans [9,10]. However, the current work focuses on a single PET/CT scan analysis to provide relevant oncological prognostic quantitative indicators.

Therefore, the authors consider that an appropriate information source for assessing the performance of the proposed PGOSIs is a specialist-based visual PET evaluation of each patient's oncological state from a consensus of independent experts in the field. In this work, we present a set of quantitative PGOSIs and test their impact at the clinical level by comparing their performance with the corresponding qualitative evaluation carried out by nuclear medicine specialists. We emphasize on the time-efficiency aspect of PGOSI computations by comparing expert-guided semiautomatic strategies and completely automatic approaches.

Materials and methods

The proposed framework for the performance assessment of PGOSI candidates in breast cancer patients is as follows. A set of 100 WB PET/CT scans corresponding to breast cancer patients with different tumor stages were acquired from the Nuclear Medicine Department at Hospital de Sant Pau (Barcelona, Spain) following all international PET/CT imaging acquisition protocols.

Fig. 1

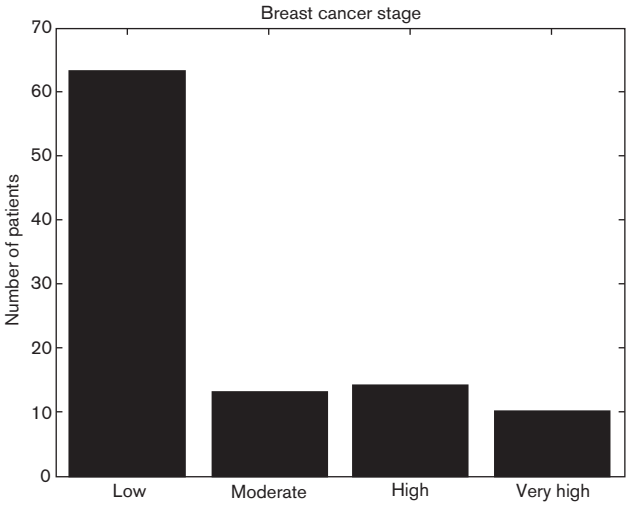

Cancer stage distribution (low, moderate, high, very high) of the patient samples.

These patients were grouped into four categories according to their tumoral state by the consensus of three independent nuclear medicine physicians as shown in Fig. 1, following visual inspection criteria. As the role of the proposed PGOSIs would have a major clinical impact on the prognosis and management of early-stage cancer patients [11], a larger number of patients in this stage were acquired.

Also, semiautomatic segmentation of metabolic tumor volume obtained from all WB PET scans was carried out by three independent nuclear medicine physicians, which yielded three independent segmentations (S1, S2, and S3) of all patients in order to test the efficacy of any PGOSI proposal in this procedure (Fig. 2). The segmentation was accomplished using a specific-purpose WB PET segmentation software tool.

To be able to test the performance of any given PGOSI proposal, the set of 100 patients was ordered according to their oncological state upon agreement among three independent nuclear medicine experts. The set of clinical variables that were taken into consideration by the experts during the ordering procedure were:

(1) C1: Total tumor volume.
(2) C2: Global aggressiveness of the tumor.
(3) C3: Spread of the tumor – that is, number of organs affected by the tumor and the number of metastases.

Now, given a PGOSI calculation proposal, once computed to the whole set of breast cancer patients, an ordering

Fig. 2

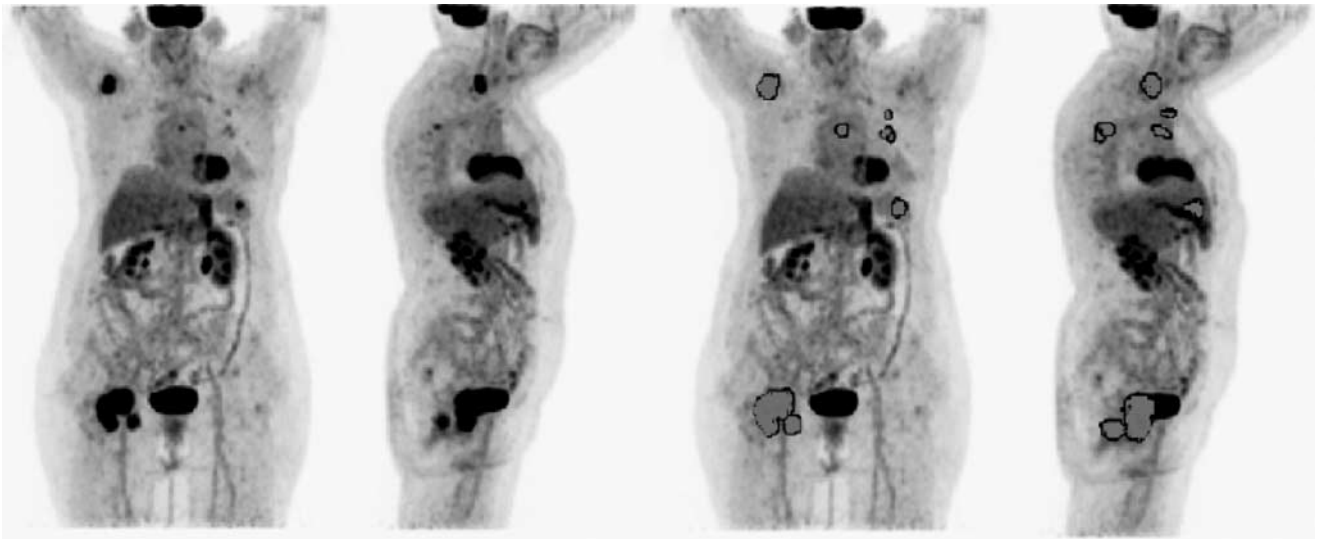

Sample metabolic tumor volume segmentation carried out by a nuclear medicine expert.

of patients according to their PGOSI value can be obtained. The performance (related to clinical impact) of the proposed PGOSI can be addressed by computing the correlation value between the experts' patient ordering and the proposed PGOSI ordering. Figure 3 shows an ordering example of a subset of the breast cancer patients, as well as the corresponding schematic drawings that have been used throughout this paper to illustrate the set of PGOSI proposals and their performance.

The set of PGOSI proposals in this work is detailed as follows. First, it should be noted that, in order to maximize performance, any PGOSI proposal should seek to quantitatively represent the clinical variables that define a patient's tumoral state (C1, C2, and C3). Second, an important property of any PGOSI should be its level of independence from any specialist evaluation, in the sense that an ideal PGOSI should be automatically computed from any given WB PET/CT scan. However, current technology is unable to automatically identify and segment the entire tumoral volume in a given WB PET/CT scan in a reliable manner (although encouraging results have been shown recently in this respect [12]). Thus, in this work we conduct a comparative analysis of the performance of the PGOSI proposals when they are computed in a completely automatic manner or after providing an expert-guided semiautomatic tumor segmentation mask. In doing this, we assume that technological advances will at some point bring both performances to the same level.

The set of existing clinically justified PGOSI proposals that are related to C1 and C2 have been already mentioned (SUV_{max}, SUV_{mean}, WBMTV, and TLG). The SUV_{max} and SUV_{mean} of the patient's whole-body tumor volume try to measure the cancer aggressiveness but miss the information related to the actual tumor quantity that is present within the patient's body. In contrast, WBMTV does measure the cancer quantity but fails to model its aggressiveness. TLG takes into account both the quantity and aggressiveness of the patient's cancer, but fails to reveal its spread (C3). The limitation of this set of PGOSIs is illustrated in Fig. 4.

To overcome these limitations, a new set of PGOSIs is proposed and described as follows. A key issue to be addressed is how to quantify the cancer spread throughout the patient's body (C3) and compare it with that of other patients, assuming that all of them have the same tumor quantity and the same mean aggressiveness. In particular, a major goal is to be able to distinguish between both tumoral conditions seen in Fig. 4d.

A first alternative would be to compute the number of connected components (NCC) [13] from the PET tumor segmentation mask, which will be related to the number of tumor lesions within the patient's body. This parameter would give a clue about the cancer spread but suffers from some limitations in the special case of a relatively condensed group of tumor lesions, wherein it could be argued that the overall cancer spread would be inferior and therefore the PGOSI value would be so. This limitation is shown in Fig. 5.

To avoid this problem, the NCC value could be combined with the average distance between components, which can be computed by averaging the distance (measured in millimeters, for instance) between the middle points of all connected components. Setting up a new parameter

Fig. 3

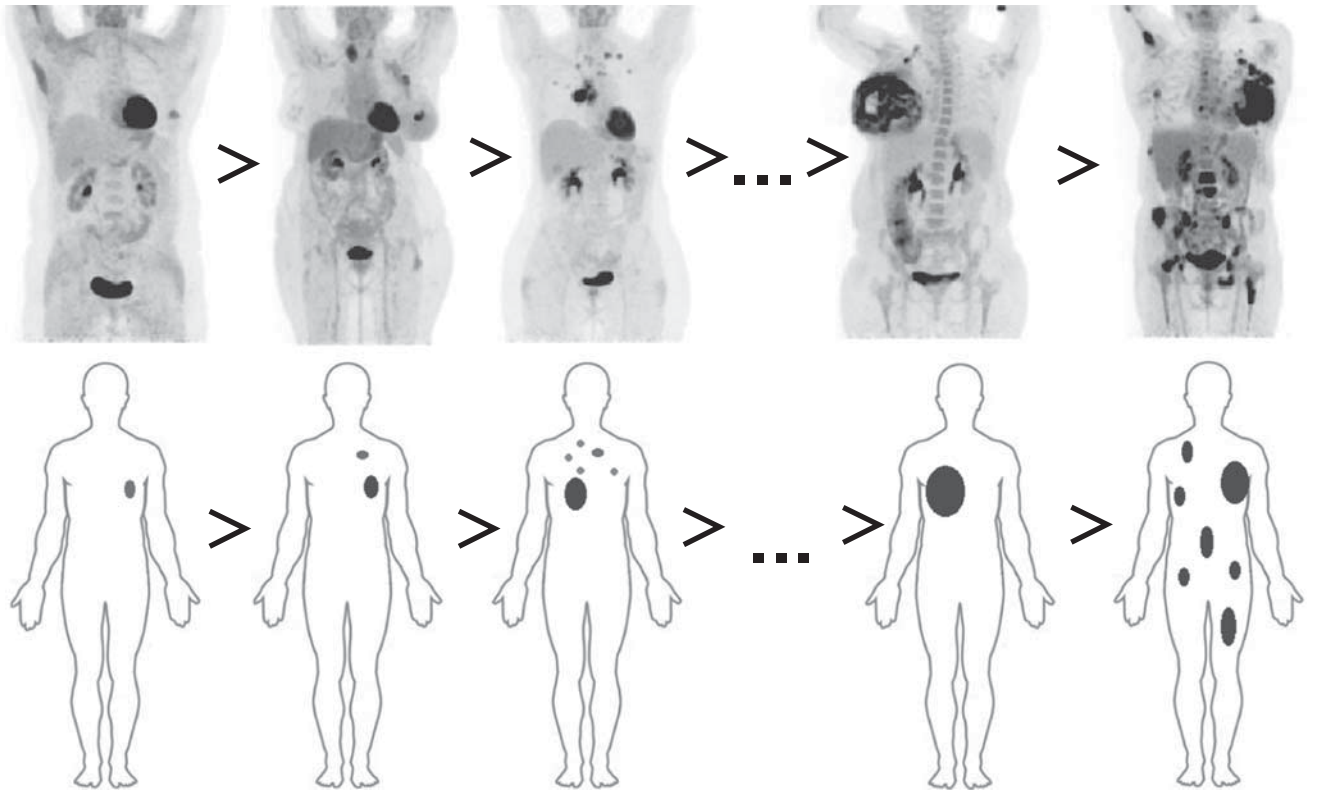

Experts' patient ordering in ascending tumoral grade based on clinical visual and semiquantitative variables (top). Schematic illustrations that model the corresponding tumor distribution within each patient's body (bottom) and its aggressiveness (represented by its grayscale intensity: the darker the higher).

based on the product of NCC and average distance between components (aNCC) overcomes the NCC limitation, but produces another limitation related to the average operation, as illustrated in Fig. 6.

One could try to extend this reasoning by introducing the SD between the middle points of the connected components as a new parameter to be taken into account. However, it rapidly becomes clear that what is needed is a new parameter that approximates the number of organs where the cancer is present within the patient's body. Note that this parameter, referred to as NORG, would overcome the limitations of NCC and aNCC (Fig. 7).

To deal with this task, the following algorithm for obtaining an approximation of the number of affected organs (NORG) is proposed. We start by setting NORG at 0. Then, for each connected component of the PET tumoral segmentation mask, if it has an average HU value significantly different from that of all other connected components or if its middle point is significantly far away from the rest of the connected components, we increase its value by 1. When terminated, an approximation of the actual number of organs or distinct anatomical locations where the tumor is present is obtained. This method has shown a positive correlation of 41% when compared with the NORG value for the 100 breast cancer patients with the actual number of affected organs identified by the medical experts for each patient (where ganglionar adenopathies were considered a single organ except if there existed superior and inferior instances). This result, which is superior to the NCC (31%) or aNCC (33%) correlation, is considered appropriate for quantitatively modeling the patient's cancer spread.

Once a set of several quantitative variables that try to measure the cancer spread has been introduced, to obtain a robust PGOSI proposal, the data obtained from it should be combined with the variables that are related to tumor quantity and aggressiveness.

A first step consists of combining the tumor quantity and aggressiveness indicators. TLG has already been proposed for this task, but the authors consider this parameter highly dependent on the segmentation procedure (as it directly includes the WBMTV) and does not consider the distribution of SUVs across all tumor regions (as it includes only the SUV_{mean}).

Fig. 4

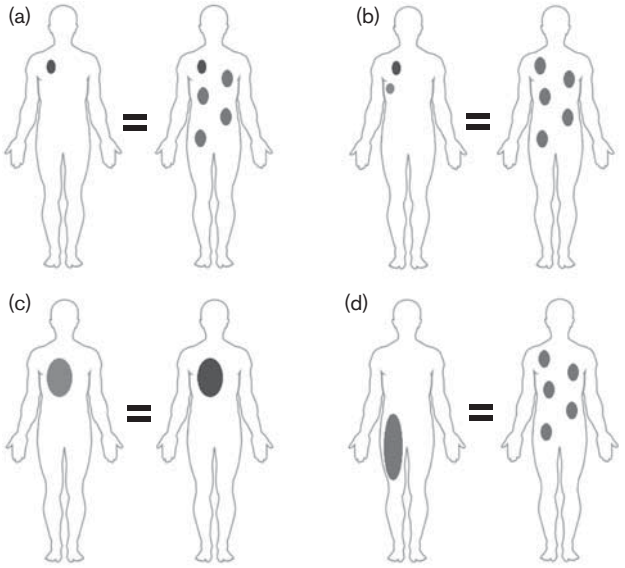

Conceptual limitations of common follow-up indicators when used as a PGOSI. The patients' schematic illustrations are based on those defined in Fig. 3. For each case, the equals sign illustrates that the same PGOSI value would be obtained in both patients [(a) SUV_{max}; (b) SUV_{mean}; (c) WBMTV; (d) TLG], albeit possessing an arguably different oncological state. PGOSI, PET Global Oncological State Indicator; SUV, standard uptake value; TLG, total lesion glycolysis; WBMTV, whole-body metabolic tumor volume.

Fig. 5

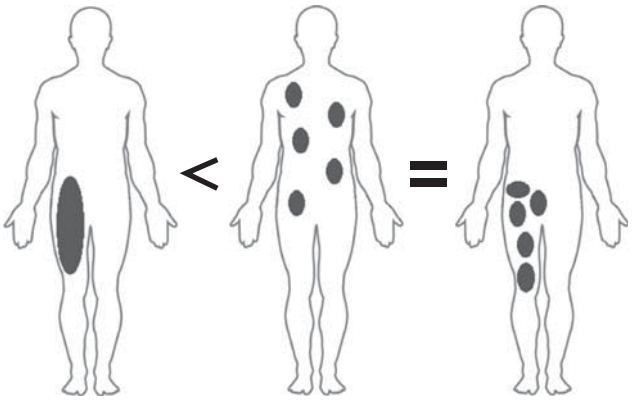

Limitation of the NCC as a measure of cancer spread. Assuming the same tumoral volume and SUV_{mean}, the NCC parameter is able to distinguish between a single big lesion and a set of smaller lesions, but does not give a clue about their spatial distribution, leading to possible clinical miss-ordering. NCC, number of connected components; SUV, standard uptake value.

Thus, a new parameter for this measurement is introduced as the sum of all SUVs of the tumor segmentation mask voxels. We consider this number to be less sensitive to the chosen segmentation method as the boundary voxels in tumor lesions (which is generally

Fig. 6

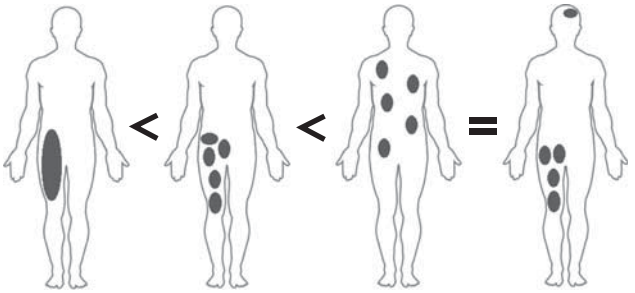

Limitation of the aNCC parameter as a measure of cancer spread. Although it succeeds at distinguishing between common spread differences, the average distance measure could lead to some miss-orderings, as it could be argued that the last tumoral state would be inferior to the third (where the tumor has reached a larger number of distinct anatomical locations).

Fig. 7

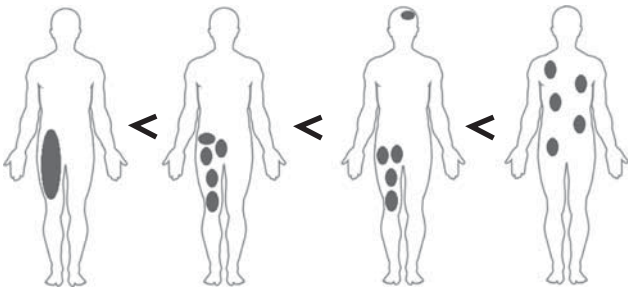

The NORG parameter as a good conceptual indicator of cancer spread across the patient's body.

responsible for the difference among segmentation methods) will contribute less to the final parameter value, as they tend to have a lower SUV. Also, taking the sum and not the average of all tumor SUVs will provide a better sense of distribution of its aggressiveness. This parameter is then normalized by voxel size (in mm^3) and the patient's body surface area, which can be easily obtained from the DICOM scan metadata. We will refer to this described parameter as nTSUV.

Before addressing the performance results of the set of PGOSI proposals, note that its derivation and analysis have been highly simplified, in the sense that in some PET/CT scans its values could be substantially altered by physiological and pathological phenomena. For instance, SUV_{max} and SUV_{mean} may be altered because of muscular uptake (Fig. 8a) or partial volume effects if the lesions are located near brown fat uptake (Fig. 8b) [14]. Also, segmenting false-positive or false-negative ^{18}F-FDG uptakes (e.g. inflammation) could alter most of the indicators, especially the WBMTV value (and even the spread indicators if a false lesion is significantly isolated from the

Fig. 8

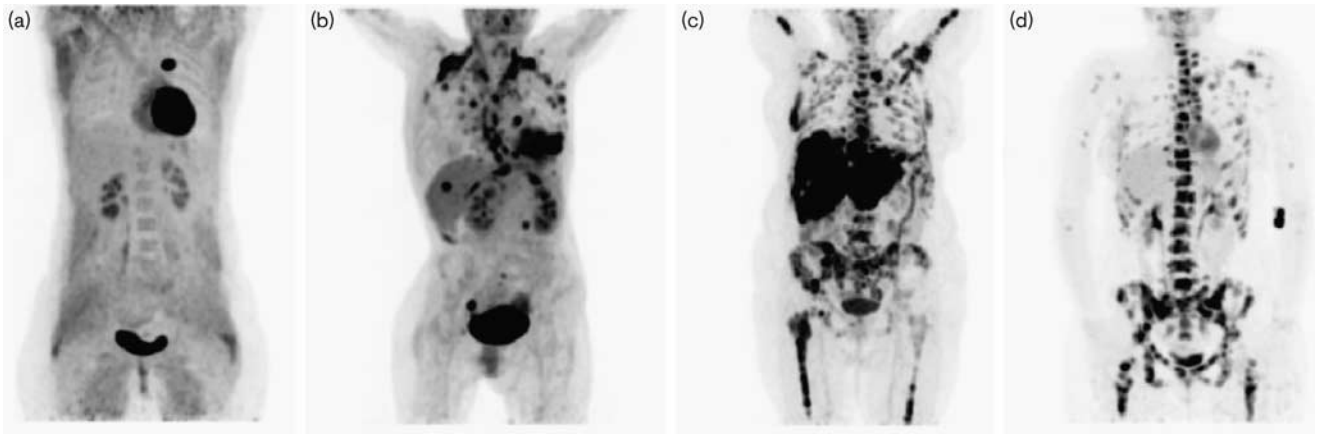

A sample of patient's physiological and pathological states that could alter any PGOSI performance. (a) muscular uptake, (b) brown fat uptake, (c and d) advanced tumoral stage. PGOSI, PET Global Oncological State Indicator.

Table 1 Performance results using Pearson's correlation coefficient of a set of PET Global Oncological State Indicator proposals

	Manual segmentation					Auto segmentation	
PGOSI	S1	S2	S3	Mean	SD	MLF	Threshold
SUV_{mean}	0.4929	0.4698	0.4945	0.4857	0.0138	0.3319	0.2492
SUV_{max}	0.5965	0.6142	0.6142	0.6083	0.0102	0.4502	0.2487
WBMTV	0.7997	0.8124	0.8040	0.8054	0.0064	0.5664	0.3154
TLG	0.7934	0.8015	0.7944	0.7964	0.0044	0.5730	0.2733
nTSUV	0.8024	0.8074	0.8026	0.8041	0.0028	0.5759	0.2562
nTSUV*NCC	0.8581	0.8561	0.8528	0.8557	0.0027	0.6214	0.2567
nTSUV*aNCC	0.8429	0.8392	0.8384	0.8402	0.0024	0.6114	0.2563
nTSUV*NORG	0.8712	0.8597	0.8642	**0.8650**	0.0058	**0.6351**	0.2578

Maximum correlation values are highlighted in bold.
MLF, machine learning framework; PGOSI, PET Global Oncological State Indicator; SUV, standard uptake value; TLG, total lesion glycolysis; WBMTV, whole-body metabolic tumor volume.

rest). Finally, the NCC, aNCC, and NORG parameters may not accurately model what they are intended for in advanced tumoral states, as seen in Fig. 8c and d. Since the experts' visual evaluation is not conditioned on these quantitative parameter variabilities, this could reflect a first limitation of the proposed PGOSI framework.

In the next section, an exhaustive performance analysis of a set of PGOSI proposals is presented. All PGOSI proposals were obtained by combining the previously described parameters, which seek to quantify the qualitative information that the medical experts use to evaluate the patients' global oncological state from WB PET/CT scans.

Results and discussion

In this section, performance results of a set of PGOSI proposals in terms of the Pearson correlation coefficient of the experts' ordering of the 100 breast cancer patients and the ordering obtained from the computation of each PGOSI are addressed.

Table 1 shows the correlation results of a set of PGOSI proposals. Performance using either manual (i.e. expert guided) or automatic tumor segmentation techniques is presented. For the manual segmentation scenario, to evaluate the segmentation independence of all PGOSI proposals, performance results are computed in three different tumor segmentation masks segmented by three independent nuclear medicine physicians (S1, S2, and S3). Completely automatic tumor segmentation strategies include the machine learning framework (MLF) described by Sampedro *et al.* [12] and a naïve direct thresholding method at an SUV of 3.0 [15].

First, note the performance results of the state-of-the-art indicators. As predicted in the previous section, the SUV_{mean} (48%) and SUV_{max} (60%) do not model a patient's global tumoral state precisely. The WBMTV and TLG parameters, as expected, give much better results (80%). These results are consistent with those obtained in clinical studies [16–18]. It is to be noted that our proposed nTSUV indicator gives the same correlation performance (80%) but is up to three times more

independent of the manual segmentation used, which is consistent with its design and proposal.

Therefore, the authors consider that the indicator that best models the quantity and aggressiveness of the tumor is the nTSUV. Now, this parameter should be combined with the spread indicators NCC, aNCC, and NORG to improve the performance results. As can be observed, a significant improvement of 6% correlation was achieved. Although no significant difference is shown regarding the use of NCC, aNCC, and NORG, the best performance results were obtained by combining nTSUV and NORG, which is consistent with the derivation presented in the previous section.

Regarding the results obtained using a completely automatic segmentation scenario, because of the high complexity of the problem, significantly lower correlation results were obtained. Very poor correlation ($< 32\%$) was obtained using the direct thresholding method, which is consistent with the fact that this method would consider any voxel with an SUV greater than 3.0 as tumoral, including physiological uptakes in the brain, heart, kidneys, and bladder. Moderate but significant correlation results were obtained using the MLF method (63%), which were remarkably higher than those of some state-of-the-art indicators such as SUV_{mean} and SUV_{max}. It is noteworthy that this methodology, despite showing about 20% worse performance than the best manual segmentation alternative, is much more time efficient and does not suffer from variabilities due to different segmentations obtained by different experts or software tools.

Figure 9 shows the state-of-the-art visual correlation results between the experts' ordering and each PGOSI using manual segmentation (S1). Figure 10 shows the corresponding results of the nTSUV*NORG PGOSI using either manual segmentation (S1) or automatic segmentation (MLF).

Another way of evaluating the performance of the nTSUV*NORG PGOSI could be by computing its mean number of position errors from the experts' ordering. Using manual segmentation, the value obtained was 11.3 ± 10.2, which means that on average the ordering resolution of this indicator is 11 positions. If one considers a plausible 5% of outliers due to either segmentation or experts' ordering errors, this number reduces to 9.8 ± 7.9. Considering that during the ordering process the nuclear medicine physicians agreed that there would be a mean 5–6-position variance if the ordering was carried out independently instead of by consensus, this result can be considered noteworthy. Using automatic segmentation (MLF), the results were 17.9 ± 17.0 and 15.3 ± 13.1 (if a 5% outlier is assumed).

In clinical practice, the impact of the proposed PGOSI can be addressed by establishing a numeric indicator

Fig. 9

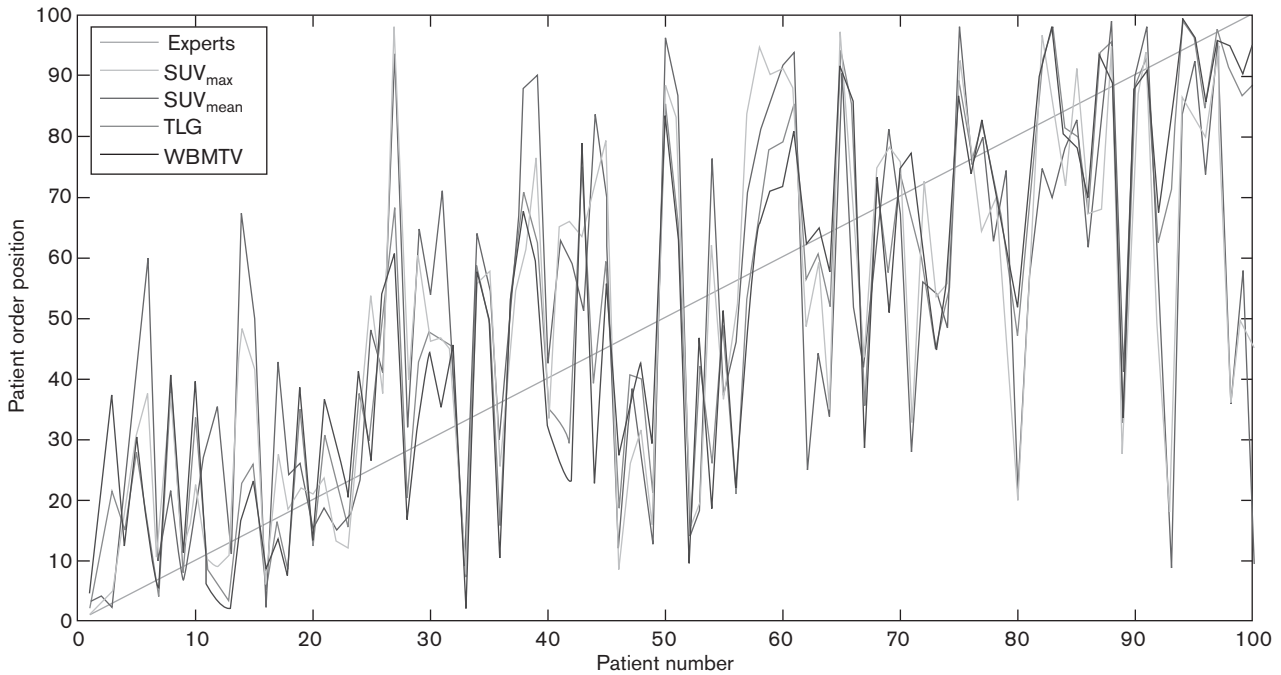

State-of-the art PGOSI performance using manual whole-body tumor segmentation. PGOSI, PET Global Oncological State Indicator; SUV, standard uptake value; TLG, total lesion glycolysis; WBMTV, whole-body metabolic tumor volume.

Fig. 10

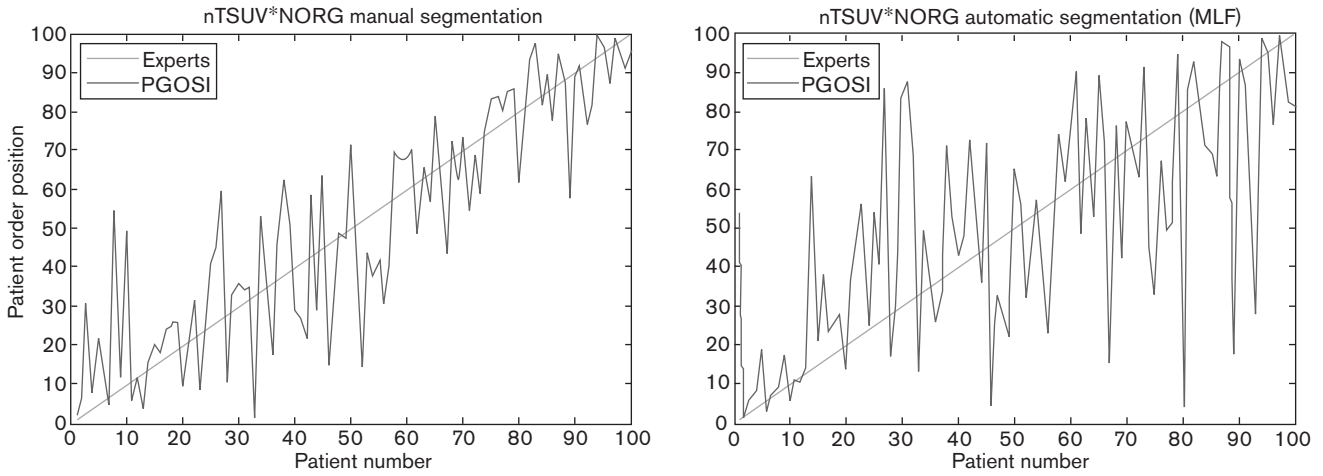

nTSUV*NORG PGOSI performance results using either manual or automatic whole-body tumoral segmentation. MLF, machine learning framework; PGOSI, PET Global Oncological State Indicator.

Table 2 Performance results using Pearson's correlation coefficient of a set of PET Global Oncological State Indicator proposals

	Manual segmentation					Auto segmentation	
PGOSI	S1	S2	S3	Mean	SD	MLF	Threshold
NCC	0.8251	0.8210	0.8255	0.8239	0.0025	0.6430	0.0012
aNCC	0.7639	0.7891	0.7753	0.7761	0.0126	0.5614	0.0025
NORG	0.8083	0.7994	0.8177	0.8085	0.0092	0.6526	0.0034
WBMTV*NCC	0.8476	0.8471	0.8523	0.8490	0.0029	0.6136	0.3174
WBMTV*aNCC	0.8370	0.8326	0.8346	0.8347	0.0022	0.6094	0.3152
WBMTV*NORG	0.8592	0.8498	0.8571	0.8554	0.0049	0.6300	0.3154
TLG*NCC	0.8519	0.8520	0.8512	0.8517	0.0004	0.6163	0.2713
TLG*aNCC	0.8420	0.8351	0.8340	0.8370	0.0043	0.6091	0.2742
TLG*NORG	0.8661	0.8524	0.8565	0.8583	0.0070	0.6334	0.2733

MLF, machine learning framework; NCC, number of connected components; PGOSI, PET Global Oncological State Indicator.

range for each of the four groups of patients based on oncological state (low, moderate, high, very high). In this case, for 90% of patients in the low group, the nTSUV*NORG value range was 21.52–5157.77; for 40% of patients in the medium group the range was 5249.52–16486.45; for 65% of patients in the high group the range was 17852.39–138386.08; and for 71% of patients in the very high group the range was 210293.92–7882691.02. These results are consistent with the difficulty of distinguishing between medium and high oncological states in a quantitative manner with a relatively small patient sample.

For the sake of completeness, Table 2 shows the performance of another set of PGOSI proposals based on the combination of other relevant indicators that have been described in this work. Although none of them achieved the performance of nTSUV*NORG, very similar performance results and tendencies were seen, which confirms that when WBMTV or TLG is combined with cancer spread indicators, a significant performance improvement is obtained.

Finally, a small illustrative test to validate the potential value of the proposed scoring system was conducted. First, the PET/CT scans of five patients (independent from the ones used in the previous analysis) with a very similar oncological state (i.e. in the same stage) were given to three independent nuclear medicine specialists to be ordered according to oncological state. As expected, the ordering varied among the specialists, and therefore the possible ordering obtained by consensus among all of them may be weak. Then, in the same setting, a new independent set of five patients in a very similar oncological state was selected. Now, however, not only images but also some of the PGOSI values for each patient (in particular, the WBMTV and nTSUV*NORG values) were provided to the specialist. A substantial agreement in the ordering by the three specialists compared with the previous scenario was

observed, which would induce a more robust ordering by consensus.

In summary, the presented results show how quantitative indicators that model the patient's oncological state from a WB PET/CT scan can be obtained such that there is significant agreement with the corresponding human-expert visual analysis. This fact represents an important contribution, as numerical indicators are known to be much more convenient in decision-making scenarios because of their robustness and human independence.

Conclusion

In this work we have presented a number of quantitative indicators computed from WB PET/CT scans that seek to model the global oncological state of a given patient. The design and performance of the proposed indicators have been addressed through a qualitative evaluation of a set of 100 breast cancer patients from a consensus of three nuclear medicine physicians. In this process, the specialists took into consideration visual and semiquantitative parameters related to the patient's tumor volume, aggressiveness, and spread. Therefore, the set of proposed quantitative indicators have been designed to model these tumor properties through the computational image analysis of the metabolic tumor volume segmentation of a WB PET scan, aiming to maximize independence from specialist evaluation.

Performance results based on the correlation between the ordering by global tumoral state of the 100 breast cancer patients performed by the consensus of experts and the proposed quantitative indicators have shown up to 87% correlation using expert-guided PET tumor volume segmentation and 64% using a completely automatic segmentation framework.

The authors consider that the results of this work have contributed to support the need of a quantitative oncological summary of a WB PET/CT scan, which would prove helpful in oncological decision-making scenarios when combined with other cancer indicators. Future work includes performing case studies in different cancer types in which PET evaluation plays a significant role (e.g. lymphoma, sarcoma, or ovarian cancer), as well as keeping track of automatic PET tumor segmentation technologies to obtain a reliable, time-efficient, and expert independent indicator computation system.

Finally, all the described framework and results will need to be validated in large cohorts in long-term studies to fully determine whether the proposed indicators are useful in oncological and nuclear medicine settings to address the prediction of the patient's outcome and treatment response.

Acknowledgements

The work of Frederic Sampedro is supported by the Spanish government FPU (Formación del Profesorado Universitario) doctoral grant. The authors express their appreciation to Professor Ignasi Carrio, Director of the Nuclear Medicine Department of the Hospital de Sant Pau (Barcelona, Spain), for providing the opportunity to develop this work.

Conflicts of interest

There are no conflicts of interest.

References

1 Hwan S, Hyup S, Young J. Prognostic significance of volume-based PET parameters in cancer patients. *Korean J Radiol* 2013; **14**:1–12.
2 Fonti R, Larobina M, Del Vecchio S, De Luca S, Fabbricina R, Catalano L, *et al*. Metabolic tumor volume assessed by ^{18}F-FDG PET/CT for the prediction of outcome in patients with multiple myeloma. *J Nucl Med* 2012; **53**:1829–1835.
3 Chung MK, Jeong HS, Park SG, Jang JY, Son YI, Choi JY, *et al*. Metabolic tumor volume of [^{18}F]-fluorodeoxyglucose positron emission tomography/computed tomography predicts short-term outcome to radiotherapy with or without chemotherapy in pharyngeal cancer. *Clin Cancer Res* 2009; **15**:5861–5868.
4 Hyun SH, Choi JY, Shim YM, Kim K, Lee SJ, Cho YS, *et al*. Prognostic value of metabolic tumor volume measured by ^{18}F-fluorodeoxyglucose positron emission tomography in patients with esophageal carcinoma. *Ann Surg Oncol* 2010; **17**:115–122.
5 Yan H, Wang R, Zhao F, Zhu K, Jiang S, Zhao W, *et al*. Measurement of tumor volume by PET to evaluate prognosis in patients with advanced non-small cell lung cancer treated by non-surgical therapy. *Acta Radiol* 2011; **52**:646–650.
6 Zhu D, Ma T, Niu Z, Zheng J, Han A, Zhao S, *et al*. Prognostic significance of metabolic parameters measured by (18)F-fluorodeoxyglucose positron emission tomography/computed tomography in patients with small cell lung cancer. *Lung Cancer* 2011; **73**:332–337.
7 Liao S, Penney BC, Wroblewski K, Zhang H, Simon CA, Kampalath R, *et al*. Prognostic value of metabolic tumor burden on (18)F-FDG PET in nonsurgical patients with non-small cell lung cancer. *Eur J Nucl Med Mol Imaging* 2012; **39**:27–38.
8 Chan W, Mak H, Huang B, Yeung D, Kwong D, Khong P. Nasopharyngeal carcinoma: relationship between ^{18}F-FDG PET-CT maximum standardized uptake value, metabolic tumour volume and total lesion glycolysis and TNM classification. *Nucl Med Commun* 2010; **31**:206–210.
9 Takeda A, Yokosuka N, Ohashi T, Kunieda E, Fujii H, Aoki Y, *et al*. The maximum standardized uptake value (SUV_{max}) on FDG-PET is a strong predictor of local recurrence for localized non-small-cell lung cancer after stereotactic body radiotherapy (SBRT). *Radiother Oncol* 2011; **101**:291–297.
10 Zhang H, Wroblewski K, Liao S, Kampalath R, Penney B, Zhang Y, Pu Y. Prognostic value of metabolic tumor burden from ^{18}F-FDG PET in surgical patients with non-small-cell lung cancer. *Acad Radiol* 2013; **20**:32–40.
11 Garami Z, Hascsi Z, Varga J, Dinya T, Tanyi M, Garai I, *et al*. The value of 18-FDG PET/CT in early-stage breast cancer compared to traditional diagnostic modalities with an emphasis on changes in disease stage designation and treatment plan. *Eur J Surg Oncol* 2012; **38**:31–37.
12 Sampedro F, Escalera S, Domenech A, Carrió I. Automatic metabolic tumor volume segmentation in breast cancer whole-body PET/CT scans: a supervised learning approach. *Med Image Anal* 2013. Under revision.
13 Biancardi A, Segovia M. Adaptive segmentation of MR axial brain images using connected components. *Lect Notes Comput Sci* 2001; **2059**:295–302.
14 Zhang H, Wroblewski K, Appelbaum D, Pu Y. Independent prognostic value of whole body metabolic tumor burden from FDG-PET in non-small cell lung cancer. *Int J Comput Assist Radiol Surg* 2013; **8**:181–191.
15 Oh J, Seo J, Chong A, Min J, Song H, Kim Y, Bom H. Whole-body metabolic tumour volume of ^{18}F-FDG PET/CT improves the prediction of

prognosis in small cell lung cancer. *Eur J Nucl Med Mol Imaging* 2012; **39**:925–935.
16 Lee P, Weerasuriya DK, Lavori PW, Quon A, Hara W, Maxim PG, *et al*. Metabolic tumor burden predicts for disease progression and death in lung cancer. *Int J Radiat Oncol Biol Phys* 2007; **69**:328–333.
17 Larson SM, Erdi Y, Akhurst T, Mazumdar M, Macapinlac HA, Finn RD, *et al*. Tumor treatment response based on visual and quantitative changes in global tumor glycolysis using PET-FDG imaging. The visual response score and the change in total lesions glycolysis. *Clin Positron Imaging* 1999; **2**:159–171.
18 Borst GR, Belderbos JS, Boellaard R, Comans EF, De Jaeger K, Lammertsma AA, Lebesque JV. Standardised FDG uptake: a prognostic factor for inoperable non-small cell lung cancer. *Eur J Cancer* 2005; **41**:1533–1541.